Research Article | Vol. 7, No. 11 | 1 Nov 2016 | BIOMEDICAL OPTICS EXPRESS 4472

Biomedical Optics EXPRESS

Terahertz identification and quantification of neurotransmitter and neurotrophy mixture

YAN PENG,[1] XIAORONG YUAN,[1] XIANG ZOU,[2] WANQING CHEN,[1] HUI HUANG,[1] HONGWEI ZHAO,[3] BO SONG,[1] LIANG CHEN,[2,5] AND YIMING ZHU[1,4]

[1]*Shanghai Key Lab of Modern Optical System, University of Shanghai for Science and Technology No. 516, Jungong Road, 200093, Shanghai, China*
[2]*Hua Shan Hospital, Fudan University, 200040, Shanghai, China*
[3]*Shanghai Institute of Applied Physics, Chinese Academy of Sciences, Shanghai 201800, China*
[4]*ymzhu@usst.edu.cn*
[5]*chenlianghs@126.com*

Abstract: Terahertz spectroscopy has been widely used for investigating the fingerprint spectrum of different substances. For cancerous tissues, the greatest difficulty is the absorption peaks of various substances contained in tissues overlap with each other, which are hard to identify and quantitative analyze. As a result, it is very hard to measure the presence of cancer cell and then to diagnose accurately. In this paper, we select three typical neurotransmitters (γ-aminobutyric acid, L-glutamic acid, dopamine hydrochloride) and two typical metabolites (inositol and creatine) in neurons to measure their terahertz spectra with different mixture ratios. By choosing characteristic absorption peaks, removing baseline and using the least square method, we can identify the components and proportions of each mixture, where the goodness of fit to practical situation is up to 94%. These results provide important evidences for identifying nerve substances and obtaining exact quantitative analysis.

OCIS codes: (300.6495) Spectroscopy, terahertz; (170.1420) Biology.

References and links

1. W. Limwikrant, K. Higashi, K. Yamamoto, and K. Moribe, "Characterization of ofloxacin-oxalic acid complex by PXRD, NMR, and THz spectroscopy," Int. J. Pharm. **382**(1-2), 50–55 (2009).
2. N. Laman, S. S. Harsha, and D. Grischkowsky, "Narrow-Line waveguide Terahertz time-domain spectroscopy of aspirin and aspirin precursors," Appl. Spectrosc. **62**(3), 319–326 (2008).
3. K. Kawase, Y. Ogawa, Y. Watanabe, and H. Inoue, "Non-destructive terahertz imaging of illicit drugs using spectral fingerprints," Opt. Express **11**(20), 2549–2554 (2003).
4. M. R. Leahy-Hoppa, M. J. Fitch, and R. Osiander, "Terahertz spectroscopy techniques for explosives detection," Anal. Bioanal. Chem. **395**(2), 247–257 (2009).
5. B. Fisher, M. Hoffmann, H. Helm, G. Modjesch, and P. U. Jepsen, "Chemical recognition in terahertz time-domain spectroscopy and imaging," Semicond. Sci. Technol. **20**(7), 246–253 (2005).
6. A. Matei, N. Drichko, B. Gompf, and M. Dressel, "Far-infrared spectra of amino acids," Chem. Phys. **316**(1–3), 61–71 (2005).
7. J. Xu, K. W. Plaxco, and S. J. Allen, "Probing the collective vibrational dynamics of a protein in liquid water by terahertz absorption spectroscopy," Protein Sci. **15**(5), 1175–1181 (2006).
8. C. S. Ponseca, O. Kambara, S. Kawaguchi, K. Yamamoto, and K. Tominaga, "Low-Frequency Spectra of Amino Acids and Short-Chain Peptides Studied by Terahertz Time-Domain Spectroscopy," J Infrared Milli Terahz Waves **31**(7), 799–809 (2010).
9. Y. Sun, Y. Zhang, and E. Pickwell-Macpherson, "Investigating antibody interactions with a polar liquid using terahertz pulsed spectroscopy," Biophys. J. **100**(1), 225–231 (2011).
10. Y. Sun, Z. Zhu, S. Chen, J. Balakrishnan, D. Abbott, A. T. Ahuja, and E. Pickwell-Macpherson, "Observing the Temperature Dependent Transition of the GP2 Peptide Using Terahertz Spectroscopy," PLoS One **7**(11), e50306 (2012).
11. A. N. Bogomazova, E. M. Vassina, T. N. Goryachkovskaya, V. M. Popik, and A. S. Sokolov, "No DNA damage response and negligible genome-wide transcriptional changes in human embryonic stem cells exposed to terahertz radiation," Sci. Rpe-UK **5**, 7749–7755 (2014).
12. P. C. Ashworth, E. Pickwell-MacPherson, E. Provenzano, S. E. Pinder, A. D. Purushotham, M. Pepper, and V. P. Wallace, "Terahertz pulsed spectroscopy of freshly excised human breast cancer," Opt. Express **17**(15), 12444–12454 (2009).

#272889 http://dx.doi.org/10.1364/BOE.7.004472
Journal © 2016 Received 1 Aug 2016; revised 3 Oct 2016; accepted 3 Oct 2016; published 6 Oct 2016

Biomedical Optics EXPRESS

13. K. Meng, T. N. Chen, T. Chen, L. G. Zhu, Q. Liu, Z. Li, F. Li, S. C. Zhong, Z. R. Li, H. Feng, and J. H. Zhao, "Terahertz pulsed spectroscopy of paraffin-embedded brain glioma," J. Biomed. Opt. **19**(7), 077001 (2014).
14. C. B. Reid, A. Fitzgerald, G. Reese, R. Goldin, P. Tekkis, P. S. O'Kelly, E. Pickwell-MacPherson, A. P. Gibson, and V. P. Wallace, "Terahertz pulsed imaging of freshly excised human colonic tissues," Phys. Med. Biol. **56**(14), 4333–4353 (2011).
15. Y. C. Sim, J. Y. Park, K. M. Ahn, C. Park, and J. H. Son, "Terahertz imaging of excised oral cancer at frozen temperature," Biomed. Opt. Express **4**(8), 1413–1421 (2013).
16. B. Vasić, S. Lavrnic, D. Damjanovic, D. Dzelebdzic, and I. Nikolic, "Myo-inositol/Creatine ratio in the differentiation of brain astrocytomas grade II and grade III," J. Neurophysiol. **53**(53), 926–939 (1985).
17. B. K. Sarkar, C. Chakraborty, A. R. Sharma, K. J. Bae, G. Sharma, G. P. Doss, D. Dutta, S. Ding, B. Ganbold, J. S. Nam, and S. S. Lee, "Novel biomarker for prostate cancer diagnosis by MRS," Front. Biosci. (Landmark Ed.) **19**(7), 1186–1201 (2014).
18. Y. Ueno, R. Rungsawang, I. Tomita, and K. Ajito, "Quantitative measurements of amino acids by terahertz time-domain transmission spectroscopy," Anal. Chem. **78**(15), 5424–5428 (2006).
19. G. Liu, Z. Zhang, S. Ma, H. Zhao, X. Ma, and W. Wang, "Quantitative measurement of mixtures by terahertz time-domain spectroscopy," J. Chem. Sci. **121**(4), 515–520 (2009).
20. J. A. Spencer, E. H. Jefferson, A. S. Hussain, D. Newnham, and T. Lo, "Tablet content analysis using terahertz transmission spectroscopy," Pharm Innov **2**(1), 18–22 (2007).
21. Z. Yan, D. Hou, P. Huang, B. Cao, and G. Zhang, "Terahertz spectroscopic investigation of L-glutamic acid and L-tyrosine," Meas. Sci. Technol. **19**(1), 158–160 (2007).
22. M. Kelley, "Terahertz time domain spectroscopy of amino acids and sugars," Dissertations & Theses – Gradworks 2013.
23. M. Franz, B. M. Fischer, and M. Walther, "The christiansen effect in terahertz time-domain spectra of coarse-grained powders," Appl. Phys. Lett. **92**(2), 021107 (2008).
24. M. Kaushik, W. H. Ng, B. M. Fischer, and D. Abbott, "Mitigating scattering effects in THz-TDS measurements," International Conference on Infrared Millimeter & Terahertz Waves, **49**(8), 1–2 (2010)
25. Y. C. Shen, P. F. Taday, and M. Pepper, "Elimination of scattering effects in spectral measurement of granulated materials using terahertz pulsed spectroscopy," Appl. Phys. Lett. **92**(5), 051103 (2008).
26. M. Kaushik, B. W. H. Ng, B. M. Fischer, and D. Abbott, "Terahertz scattering by granular composite materials: An effective medium theory," Appl. Phys. Lett. **100**(1), 011107 (2012).

1. Introduction

Terahertz (THz) range refers to the far infrared electromagnetic waves with frequency between 0.1 and 10 THz, or wavelength between 0.03 and 3 mm. Its radiation occupies a middle ground between microwaves and infrared light waves, which is a transition region from the electronics to photonics. Recent years, with the aid of ultrafast laser, THz technology have been widely applied to the testing of medicines [1,2], drugs [3–5] and biomolecules [6–10]. Furthermore, since THz waves have very low photon energy, it will not damage the morphology of chromosome and cells, or the DNA double helix structure, mitotic division and the functions of stem cells [11]. Therefore, people show more interest on the application of THz technology to biology and medicine in recent years, especially the cancer tissues identification [12–15].

It has been known that in the real tissue cells, substances are mixed with each other, where the proportions between them can reveal the status of tissue cells. For instance, the ratio of creatine and inositol can show the lesion status of cells [16], the metabolite ratios such as citrate (Cit)/choline (Cho) can reveal the benign prostatic hyperplasia (BPH) and prostatic cancer (PC) [17]. Then, many research groups want to realize the quantitative analysis of the mixtures and finally the early diagnosis of cancers [18–20]. However, all of these experiments have only tested binary and ternary substances mixtures and the relative errors of unclear spectra have an obvious increase from 11% to 20% while the concentration of components decrease [18]. These results have provided some proofs for quantitative analysis of mixtures but not enough for the practical application.

For human's brain, the tissue cells contain thousands of substances, but only several of them will have concentration change when diseases occur, such as γ-aminobutyric acid (GABA), L-glutamic acid (L-Glu), dopamine hydrochloride (DH), D-myo-inositol (D-MI) and creatine monohydrate (CMH)). L-glutamate is most frequently used at excitatory synapses throughout the central nervous system. GABA is the major transmitter of various inhibitory neurons and interneurons in the brain. In human body, GABA could be synthesized

Biomedical Optics EXPRESS

from glutamate in a reaction catalyzed by glutamic acid decarboxylase. In the brain, dopamine functions as a neurotransmitter, several important diseases of the nervous system are associated with dysfunctions of the dopamine system, and some of the key medications are used to treat them by altering the effects of dopamine. Myo-inositol plays an important role as the structural basis for a number of secondary messengers in eukaryotic. Creatine is a nitrogenous organic acid that occurs naturally in vertebrates and helps to supply energy to all cells in the body. For these five substances, some spectral and quantitative analysis has been done [6,21,22]. However, the spectral width and accuracy are very limited. Therefore, further work about the wider spectrum and the higher analysis precision are urgently needed.

In this paper, by improving the signal to noise ratio (SNR) of spectrum, eliminating the baseline in the experimental measurement, and combining the least square method (LSM), we can effectively identify the components in mixture and the proportion of each substance, where the goodness of fit to practical situation is 97%, 95% and 94% for mixtures of two, three and four substances, respectively.

2. Experiment

The absorbance spectra of these five substances were obtained on pressed tablets of polycrystalline powders. The powders were purchased from Sigma-Aldrich Corporation and used without further purification [purity>99%, particle sizes are smaller than that of polyethylene (~50 μm) after the grinds). These substances were stored according to the indications of the supplier. Each neuron was mixed with polyethylene (PE) and then pressed as 13 mm tablet with a force of 3 ton. The masses of all tablets are controlled to 100 mg (the mass ratio between material and PE is 1:19) and the mass lost are controlled less than 1%. The measuring accuracy was controlled to ± 0.2 mg and each spectrum was averaged 32 times. The thicknesses of the resulting tablets (typically around 450 μm) were measured by a micrometer. In order to avoiding the damage of substances, we controlled the grinding force and the pressing time strictly around 1 minute. The absorbance spectra were measured by Fourier Transform Infrared Spectrometer (FTIR) [Bruker VERTEX 80v], whose resolution is 0.001 THz and SNR is 40000:1. All the experiments were performed at room temperature (~22°C).

Based on the recorded transmission spectra of tablets, we calculated the absorbance coefficient A in the following way:

$$A = log(\frac{T_s}{T_R}) \tag{1}$$

T_s is the transmission measured through the sample tablet and T_R is the transmission measured through the PE tablet with the same mass.

According to the measured spectrum, we could assume that in a mixture model, the absorbance coefficient of each sample could be illustrated as a matrix, n is defined as the data points across the frequency range of the spectrum. In this paper, the absorbance coefficient matrix of L-Glu is formed as $\boldsymbol{O_L}$, D-MI is formed as $\boldsymbol{O_D}$, CMH is formed as $\boldsymbol{O_C}$ and GABA is formed as $\boldsymbol{O_G}$, mixture could be formed as $\boldsymbol{O_M}$.

Therefore, the principle of quantitative analysis could be written as:

$$\boldsymbol{k} * \boldsymbol{O_T} = \boldsymbol{O_M} \tag{2}$$

where $\boldsymbol{k}$ which is a $\mathbf{1} \times \mathbf{4}$ matrix represents the ratio and $\boldsymbol{O_T}$ represents a $\mathbf{4} \times \mathbf{n}$ matrix which contains the four standard pure spectra. These two parameters are showed in Eq. (3) and Eq. (4):

$$\boldsymbol{k} = (\boldsymbol{k_L}, \boldsymbol{k_D}, \boldsymbol{k_C}, \boldsymbol{k_G}) \tag{3}$$

Biomedical Optics EXPRESS

$$\boldsymbol{O}_T = \begin{pmatrix} \boldsymbol{O}_L \\ \boldsymbol{O}_D \\ \boldsymbol{O}_C \\ \boldsymbol{O}_G \end{pmatrix} \tag{4}$$

In Eq. (3), $\boldsymbol{k}_L$, $\boldsymbol{k}_D$, $\boldsymbol{k}_C$ and $\boldsymbol{k}_G$ represent the calculated factors of L-Glu, D-MI, CMH and GABA respectively.

3. Results and discussion

The absorbance spectra of these five substances are displayed in Fig. 1. The corresponding absorption peaks of each substance are labeled on each figure.

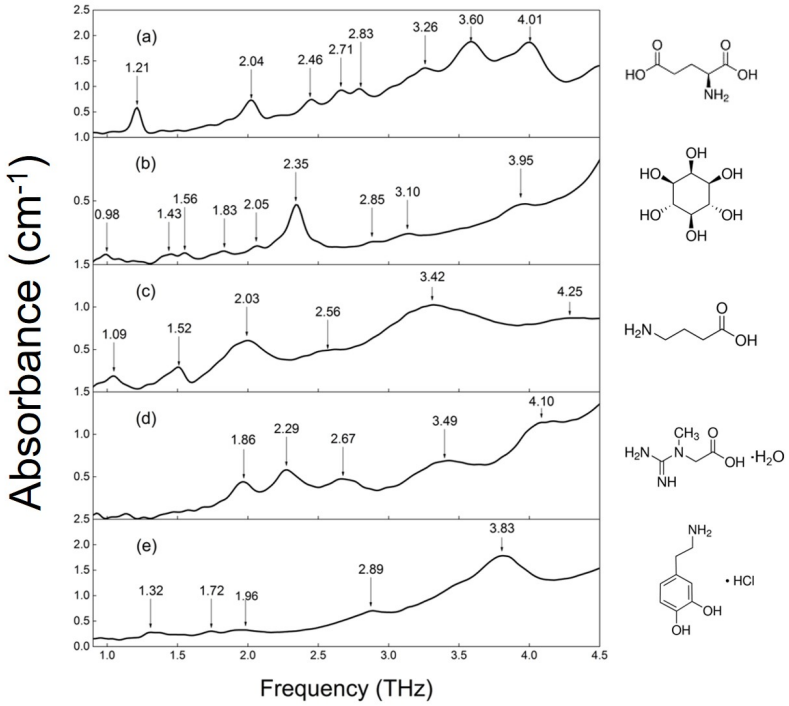

Fig. 1. THz spectrum of (a) L-glutamic acid; (b) D-myo-inositol; (c) γ-aminobutyric acid; (d) creatine monohydrate; (e) dopamine hydrochloride. Their corresponding molecular structures are listed on the right. All the absorption peaks labeled on the figures are common peaks from multiple measurements.

After obtaining the spectrum of each substance, we also measured the spectra of mixtures containing two, three and four substances, respectively.

Firstly, L-Glu and D-MI were chosen as original samples for mixed tablets, where the spectra of these two substances have obviously separate and sharp absorption peaks. It is a properly simple model for observing the relativity between the spectra of mixture and pure substances. Figure 2 shows the corresponding THz spectra. It can be seen clearly that the absorption peaks of mixture present different ratios as the mixing ratios between L-Glu and D-MI increases from 1:1 to 1:2. Additionally, we could observe that the peaks contributed by D-MI show higher amplitude when its concentration is improved and the baseline of curve have an entire lifting.

Considering the mix between different substances is linear, i.e., they don't have chemical reaction with each other, we use the LSM method to realize the ratio calculation [23–26]. Additionally, to improve the precision and accuracy, the initial spectra can be averaged many

Biomedical Optics EXPRESS

times to improve the signal-to-noise ratio (SNR), and the baseline in the spectrum should be properly removed [the detail process: For each initial spectrum, we choose minimums at different frequencies as a series reference points, then fit them by using different order polynomial based on the least square. The obtained curve is used as the absorption baseline, which will be removed from the initial spectrum. Importantly, in order to ensure the accuracy and smoothness of baseline, the sum of squares of reference points themselves and their derivatives are calculated respectively, where their values should be closer to zero]. Finally, the calculated results are shown in Table 1. The reproduced factors of D-MI to L-Glu are 0.98:1 and 0.98:2, respectively, with the root-mean-square (RMS) values of 2.27% and 1.56% as compared to the experimental ratios.

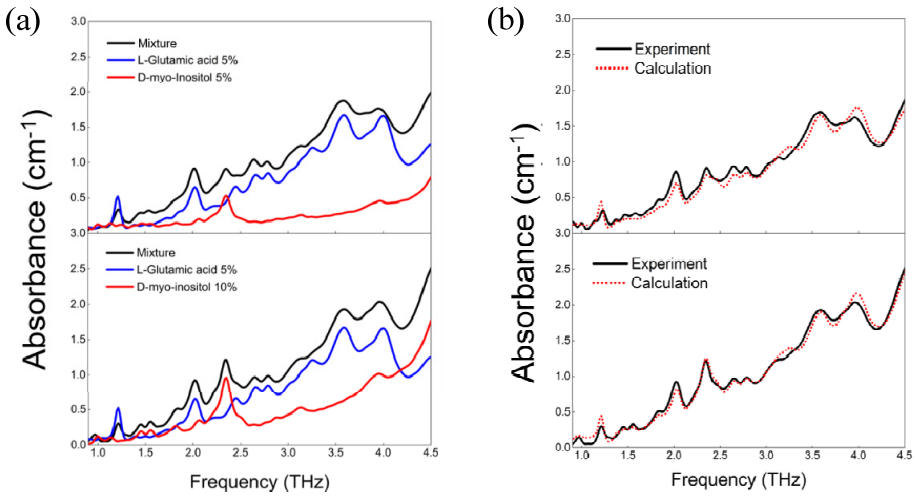

Fig. 2. The spectra of mixture made by L-Glu and D-MI (a) Experimental results of L-Glu and D-MI mixture in different ratios; (b) Experimental results and reproduced curves with calculated factors

Table 1. Quantitative analysis of L-Glu and D-MI mixture

Sample name	Concentration	Real ratio	Reproducibility	Calculated ratio	RMS	Average RMS
L-Glu	4.4%	1:1	4.27%	0.98:1	2.95%	2.27%
D-MI	4.4%		4.33%		1.59%	
L-Glu	4.5%	1:2	4.41%	0.98:2	2.00%	1.56%
D-MI	9.0%		9.01%		1.11%	

For the mixture of L-Glu and GABA, the spectra of mixture are shown in Fig. 3 and the calculated ratio are shown in Table 2. It can be seen that error of reproduced factor increases to 2.33%.

Biomedical Optics EXPRESS

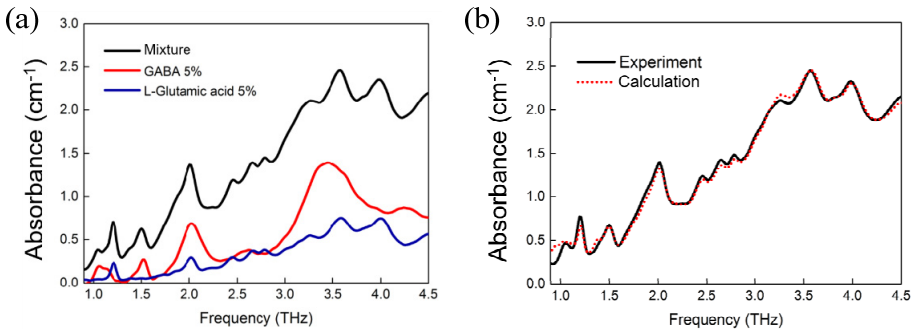

Fig. 3. The spectra of mixture made by L-Glu and GABA (a) Experimental results of L-Glu and GABA mixture; (b) Experimental result and reproduced curve with calculated factor

Table 2. Quantitative analysis of L-Glu and GABA

Sample name	Concentration	Real ratio	Reproducibility	Calculated ratio	RMS	Average RMS
L-Glu	4.35%	1:1	4.25%	1.02:1	1.16%	2.33%
GABA	4.35%		4.15%		3.49%	

Then, we chose L-Glu, D-MI and CMH for the three-component mixtures. The measured and calculated results are shown in Fig. 4 and Table 3.

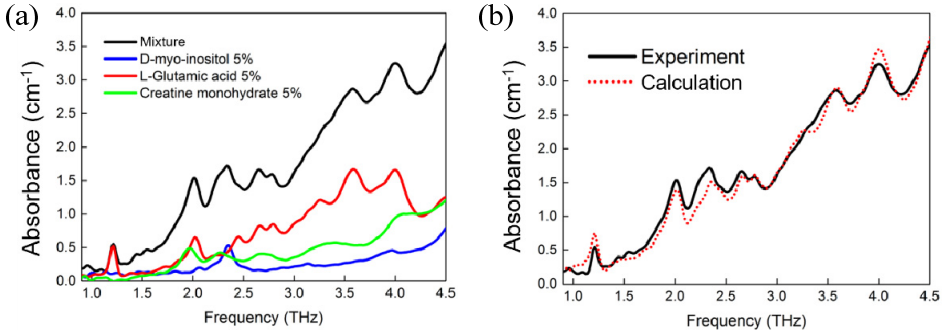

Fig. 4. The spectra of mixture made by L-Glu, CMH and D-MI (a) Experimental results of L-Glu, CMH and D-MI mixture; (b) Experimental results and reproduced curve with calculated factor

Table 3. Quantitative analysis of L-Glu, D-MI and CMH

Sample name	Concentration	Real ratio	Reproducibility	Calculated ratio	RMS	Average RMS
L-Glu	4.65%	1:1:1	4.65%	1:0.91:0.82	0.00%	4.65%
D-MI	4.65%		4.55%		2.15%	
CMH	4.65%		4.10%		11.8%	

Finally, four-component mixtures consisting of L-Glu, CMH, GABA and D-MI are also investigated, as shown in Fig. 5 and Table 4.

Biomedical Optics EXPRESS

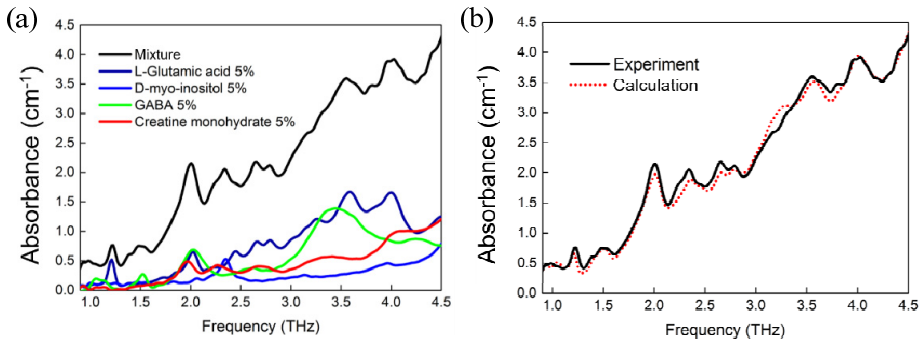

Fig. 5. The spectra of mixture made by L-Glu, CMH, GABA and D-MI (a) Experimental results of L-Glu, CMH, GABA and D-MI mixture; (b) Experimental result and reproduced curve with calculated factor

Table 4. Quantitative analysis of L-Glu, GABA, D-MI and CMH

Sample name	Concentration	Real ratio	Reproducibility	Calculated ratio	RMS	Average RMS
L-Glu	4.90%	1:1:1:1	4.50%	0.92:1:0.94:0.98	8.16%	5.44%
D-MI	4.90%		4.90%		0.00%	
CMH	4.90%		4.60%		6.12%	
GABA	4.90%		4.80%		2.04%	

Basing on all the results above, we can conclude that the accuracy for the identification and quantification of mixture are decided by four factors:

1. The shape of absorption peaks from every component in mixture. Due to that absorption peaks with larger full width at half maximum (FWHM) will increase the overlap between peaks and then increase the difficulty of identification. As a result, substances with sharper absorption peaks are easy to be identified and can induce fewer errors than that with unclear absorption peaks.

2. The SNR of measured spectra. Since the noise in every spectrum is not a constant, thus increase the SNR will reduce the uncertainty in the process of quantitative analysis.

3. Concentration of components. The lower the concentration of substance in the mixture, the corresponding absorption spectrum is more flat, i.e., the absorption peaks are harder to be recognized. Thereby, the relative error will increase quickly as the concentration ratio decreases.

4. The existence of baseline. Baseline is caused by the scattering of solid state samples in the THz region, which will break the linearity between mixtures and their components and therefore increase the difficulty of identification and quantitative analysis. Additionally, the value and complex degree of baseline will increase greatly as the types and concentrations of components increase. The baseline could be recognized as a simple quadratic function and the value of its parameter will have a clear growth along with the concentration and the type of components. Therefore, the elimination of spectrum baseline is a necessary way for improving the accuracy of quantitative analysis.

4. Conclusion

In this paper, we experimentally investigated the THz spectra of five important neurotransmitters and neurotrophy molecule including L-Glu, GABA, D-MI, CMH and DH spanning 0.9 to 4.5 THz. In order to identify the ingredient of mixture and the proportion of each substance for the aim of early diagnosis, we also investigated the spectra of mixtures

Biomedical Optics EXPRESS

made by these important neurotransmitters and neurotrophy substances. By improving the SNR of spectrum, eliminating the baseline in the experimental measurement, and combining the least square method, the average accuracy for two-component mixtures can over 97%, for three-component mixtures can over 95% and for four-component mixtures can over 94%. These research results provide an effective way for the quantitative analysis of mixture.

Funding

National Program on Key Basic Research Project of China (973 Program, 2014CB339806); Major National Development Project of Scientific Instrument and Equipment (2012YQ150092, 2012YQ14000504); Program of Shanghai Pujiang Program (16PJD033); Shanghai Zhangjiang Program (ZJ2014-ZD-004); Shanghai Subject Chief Scientist (14XD1403000); Shanghai Basic Research Key Project (14DZ1206600).